Closing the Loop via Scenario Modeling in a Time-Lapse Study of an EOR Target in Oman

*Tania Mukherjee *(University of Houston), Kurang Mehta, Jorge Lopez (Shell International Exploration and Production Inc.), Robert R. Stewart (University of Houston)*

Summary

At an EOR field in South Oman an extensive synthetic modeling study was done in order understand steam flow behaviour within the reservoir. To understand the permeability distribution within the steam flooded zone, a simulated "Close-the-Loop" workflow was executed based on scenario modeling that relates changes in acoustic properties (velocity and density) with those in reservoir properties such as oil saturation, temperature, permeability. Time-lapse zero-offset synthetic seismic were generated from a "Reference" reservoir model representing the ground truth. This synthetic seismic was used as "data" in the CtL workflow. The "Reference" model obeys all in-situ measurements including temperature logs from the observation wells. We also created a set of scenarios i.e., variances of the "Reference" reservoir model in terms of permeability distribution. Time-lapse synthetic seismic corresponding to each of the scenarios were compared with the data, in a time-lapse sense, to select a scenario most similar to the "Reference" reservoir model.

We used three approaches to compare scenario synthetics with the data: (1) similarity attribute, (2) difference of maps, and (3) difference of energy, to select the scenario that best fits the data. Seismic quantification of the match between these scenarios and the "Reference" reservoir model helped identify the scenario whose permeability distribution matches with that of the "Reference" model, in the zone of interest, and hence, Close the Loop.

Introduction

As we inject steam in a reservoir it alters its petrophysical properties (velocity,density etc) over time. Generally we look at a temperature response and try to understand flow pattern, but temperature is not uniquely related to permeability, i.e., different permeability distributions can give rise to a similar temperature profile. A preferable way to decrease the uncertainty is to consider several scenarios (dynamic reservoir models) that can give rise to the same temperature behavior in a specific EOR area and try to identify the scenario that best matches a time-lapse seismic response. We have worked out an iterative approach to "Closing the Loop" based on scenario modeling (Figure 1). In this piece of work, time-lapse synthetic seismic generated from a "Reference" reservoir model is considered as simulated "data". The synthetic seismic could be generated in various ways (zero-offset convolution with reflectivity, full wavefield propagation, etc.), as described in the right portion of the workflow in Figure 1. We have generated zero-offset convolutional synthetics. Several scenarios are also generated as variances of the same "Reference" reservoir model, in terms of permeability distribution. Similar to the "Reference" reservoir model, for each scenario, acoustic properties are computed from the reservoir properties along with rock and fluid models (Rocco *et al*., 2010). These acoustic properties are then used to compute reflectivity and further generate zero-offset synthetic seismic by convolving the reflectivity with a desired wavelet.

The process of generating synthetic seismic is carried out both for baseline (before steam injection) and monitor (after steam injection) cases and this seismic is used to generate time-lapse seismic attributes. We compare the time-lapse attributes generated from the "data" and the "scenarios" using a few approaches: 1) qualitative/visual comparison, 2) similarity attribute, and 3) difference of energy between "data" and scenario. As an outcome of this comparison, we are able to select the scenario whose synthetic time-lapse seismic response best fits the data and hence use that as the new "Reference" reservoir model or modify the existing "Reference" reservoir model to match the selected scenario. This concludes an iteration of the loop. Here we execute this loop using simulated data but the workflow can and should be exercised on field data, especially after each monitor seismic survey, to refine the reservoir model and make it most representative of the subsurface.

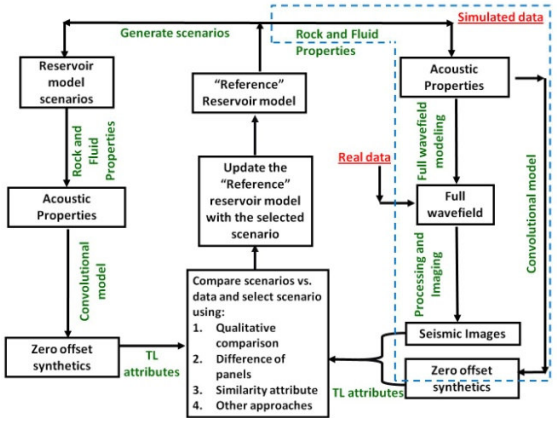

Figure 1: Schematic diagram of Closing-the-Loop through scenario modeling.

We got an opportunity to evaluate this CtL methodology in an EOR field in South Oman, where production is being enhanced by steam injection. The injection pattern is an inverted 7-spot pattern as shown Figure 2. The injector well

© 2012 SEG
DOI http://dx.doi.org/10.1190/segam2012-0804.1

(I) shown in red is situated at the center and six producer wells are situated at the six corners. The distance between adjacent producers well is 125 m.
As part of in-well surveillance program, temperature data were collected at regular time intervals. These data were used as a constraint in generating the scenarios of the "Reference" reservoir model. Temperature readings in a few producers suggested that the steam was propagating preferentially to the north, indicating the possibility of a highly permeable connection between the injector well and well P4 (Figure 2).

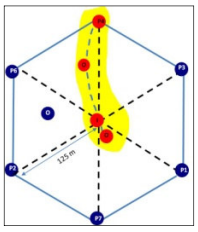

Figure 2: The steam injection pattern outline. 'P'–producer wells, 'O' – observation wells, 'I' –injector well. Red - hot wells at the time of monitor surveys.

Reservoir engineers have created a "Reference" reservoir model based on the geological information and petrophysical input from the well control points. Figure 3 shows map and profile view of the temperature front in the "Reference" reservoir model for baseline and monitor vintages. Comparison of the temperature measurements at wells with that modeled in the reservoir model indicate that they do not match. Such discrepancies inspired us to think about a few scenarios (variances of the "Reference" model) that would honor the existing temperature data. A total of 6 scenarios were generated.

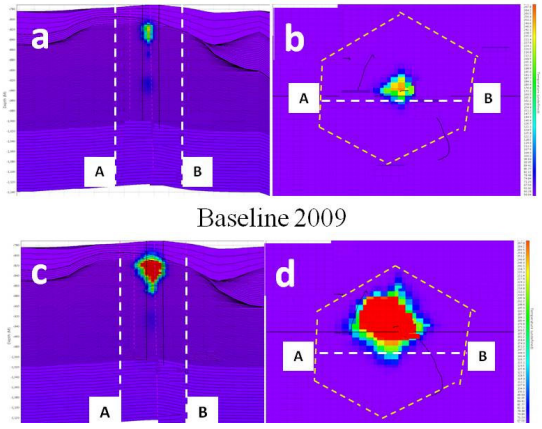

Figure 3: Temperature profiles and maps of Reference Model for two time vintages: a) temperature profile for baseline 2009, b) map view of temperature for baseline 2009 at the reservoir level, c) temperature profile for monitor 2010, and d) map view of temperature for 2010 monitor at the reservoir level.

Description and Analysis of scenarios

The six scenarios used here differ from each other and from the "Reference" reservoir model in terms of their permeability distribution or presence or absence of shale layers within the reservoir acting as baffles. Each scenario is made of layers characterized by different grid size. Once the structure is defined, we assign petrophysical values to each grid point. The terms "top thick" and "top thin" are used to describe permeability distribution in the models. In a "top thick" model, the grid size is bigger in the top layers and decreasing with depth, allowing steam to propagate more to the top and less to the bottom layers. Conversely, in a "top thin" model, the grid size is smaller at the top and increasing with depth, making steam propagate more to the deeper layers. Details for each scenario are listed below:
Scenario S2: Horizontal permeabilities for the top few layers within the reservoir are overwritten to 10 D. Such highly permeable model helps to visualize high steam within the reservoir but is not realistic.
Scenario S3: Horizontal permeabilities are modified to generate temperature profile according to the temperature log data. Scenario S3 has a top thick permeability distribution which means the permeability in shallow layers is higher than in deep layers.
Scenario S4: Horizontal permeabilities are modified to generate temperature profile according to the temperature log data but bottom horizontal permeabilities are higher to give it a top thin look.
Scenario S5: Scaled version of S3 (top think) where the absolute permeabilities of the imposed layering are reduced by a factor of 10.
Scenario S6: Scaled version of S4 (top thin) where the absolute permeabilities of the imposed layering are reduced by a factor of 10.
Scenario Sb: There are many 0.5 m thick baffles introduced, honoring the regional geology at the reservoir level.
Time-lapse acoustic properties for each of the scenarios and the "Reference" reservoir model are computed separately. After computing acoustic properties we calculated their reflectivity, which is then convolved with a source wavelet (extracted from existing surface seismic) to generate zero-offset time-lapse synthetic seismic data. The seismic generated from the scenarios are then compared against the "data" (synthetic seismic from the "Reference" model). Panels in Figure 4 show the difference between baseline and monitor seismic for our data and each of the scenarios. First look at the difference panels indicate that scenarios S3 and S4 look more like our "data" and S6 and Sb have the least similarity.

© 2012 SEG

DOI http://dx.doi.org/10.1190/segam2012-0804.1

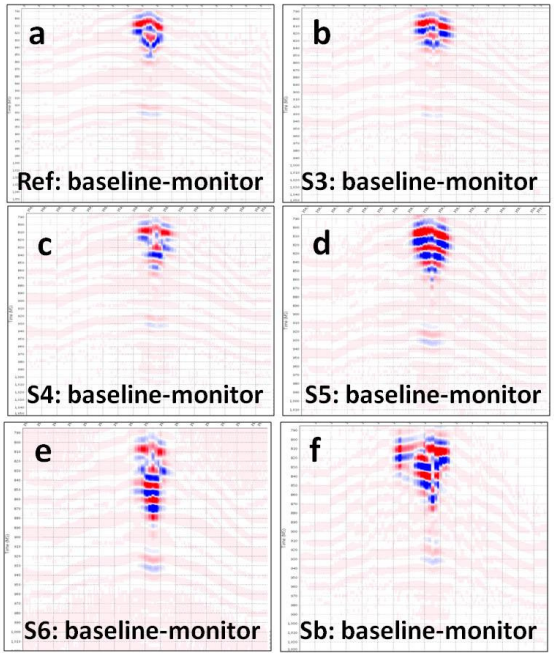

Figure 4: Difference of synthetic seismic for the baseline vintage (2009) and monitor (2010). Panels a) show the difference of seismic amplitudes for the reference model. The remaining panels show similar displays for the scenarios (Each panels are labeled accordingly S3 stands for scenario 3 where Sb is for scenario baffle)

Time lapse Analysis

After creating the baseline and monitor synthetic seismic volumes for the "Reference" model and each of the scenarios, the time-lapse responses in the form of 4D attributes were calculated. We used seven time-lapse attributes to visualize the time-lapse effects at the reservoir level:

1. Normalized RMS of amplitude difference, also known as unsigned RRR (RMS Repeatability Ratio)
2. Normalized difference of RMS amplitude, also known as signed RRR (RMS Repeatability Ratio)
3. The Difference of sum of negative amplitudes
4. The Difference of sum of positive amplitudes
5. Difference of RMS amplitudes
6. RMS of amplitude differences
7. Difference of peak amplitudes

Out of these seven attributes the first two, unsigned and signed RRR, are the most commonly looked-at time-lapse attributes. The purpose of looking at other attributes here is to illustrate that even though they may show similar shape of the time-lapse response, certain attributes are more appropriate to obtain details about the time-lapse response in some regions of interest. Given that we are working with simple time-lapse synthetic data, it suffices to look at the unsigned RRR (RMS Repeatability Ratio) – a common measure of data non-repeatability). The values of this attribute ranges from 0 (no change) to 2 (maximum change). For more complicated field dataset, it is however encouraged to analyze all of the attributes listed above for a comprehensive time-lapse analysis. The top left panel in Figure 5 shows the RRR response for our data, with no noise added. As we increase the random noise level in the data, it becomes progressively difficult to follow the steam front. This is shown in the remaining panels of Figure 5, which shows the time-lapse response for three different noise levels, corresponding to RRR values of 0.19, 0.56 and 1.4. These RRR values are representation of the SNR. As an example here we can see when we incorporate noise equivalent to RRR of 1.4, it becomes difficult to identify the boundary of the steam.

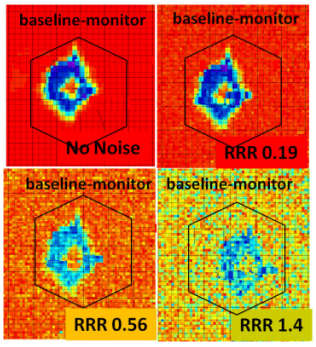

Figure 5: RRR attribute maps of time-lapse seismic data obtained from the reference model. Each panel shows the attribute map and different noise levels, characterized by RRR (labeled on each panel).

Comparison of reference data with the scenarios

Once the time-lapse attribute maps are generated for the "data" and all the scenarios, we attempt to qualitatively compare them by looking at their shape, size and amplitude distribution. For qualitative comparison we selected a time-lapse attribute (unsigned RRR) and visually compared the map for each scenario with that for our data. Visual comparison in both map and profile view suggested that scenario S4 is the most similar to our data. Apart from visual comparison, three methods of quantification were used:

1.Similarity attribute
2.Subtraction of maps
3.Difference of energy

The similarity attribute approach has been discussed by Fomel and Jin (2009). This method gives a value of similarity between two data volumes or maps by computing the normalized zero-lag cross-correlation between them. The value ranges between -1 (perfectly co relatable but opposite polarity data) to 1 (perfectly similar). Figure 6 plots the similarity attribute for each of the scenarios as compared to our data for the monitor case. There are two

© 2012 SEG

DOI http://dx.doi.org/10.1190/segam2012-0804.1

similarity curves, one for the comparison of attribute maps and one for comparison of seismic volume difference. For example, the similarity attribute for maps of scenario S2 with our data is about 0.83. Similarly values for each scenario, both for map and volume comparison, are computed and plotted. Such analysis suggests that scenario S6 is the most correlated to the simulated data, only slightly better than scenario S5. Volume comparison, however, suggests that scenarios S4 and S2 are most similar to the simulated data. Given that our interest is generally in the region of injection (around top reservoir level) and not in the entire reservoir column, we give more weight to the results from the map views; here S6 is the best fit, counter-intuitive to the first-look observation. As the random noise level is increased to RRR=0.19, 0.56 and 1.4, the selection of the best matching scenario using similarity value remains the same, although selection becomes increasing difficult.

Another approach to comparing synthetic seismic from scenarios with the simulated data is to difference one time-lapse attribute map from the other and computes the residual energy (quantified by the normalized root mean square of the residual energy). When the two maps in comparison are more like each other, the residual energy is less. Figure 7 suggests that out of all the six scenarios, the residual energy for scenario S6 is the least, both visually and in terms of its RMS value. This suggests that according to the "difference of maps" approach scenario S6 also appears to be the most similar to our data.

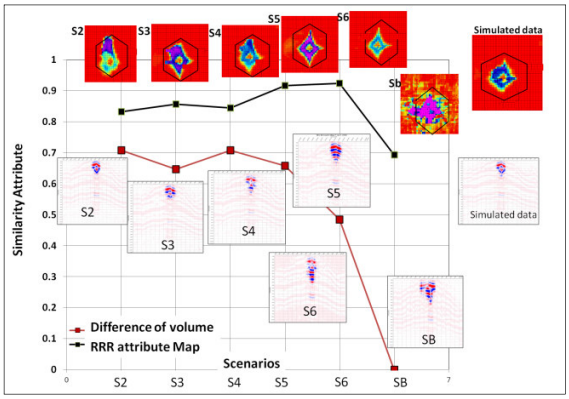

Figure 7: Plot of similarity attribute, for no noise case, as a function of scenarios. The two curves show similarity measure (in volume and map respectively) of the data from the reference model and the scenarios. The attribute maps and amplitude difference volumes that were used to compute the similarity attribute are shown for each scenario and the reference data.

Conclusions and Future work

We executed a detailed workflow to Closing-the-Loop (CtL) using synthetic data for a steam injection oil field in South Oman. We were able to select a scenario S6 as the closest to our data. This selection was possible after careful quantitative comparison and counter-intuitive to the first-look observation. So we illustrate that 1) it is very important to consider a range of realistic scenarios which can give a similar temperature effect, and 2) scenario-based Closing-the-Loop when carried out properly helps identify the scenario that best honors the data, which may be counter-intuitive to the first-look observations. We were able to set up a quantitative CtL workflow that helps select the most suitable reservoir model. We tried two quantitative approaches for attribute comparison and concluded that both the similarity attribute and difference of RRR energy plot work consistently with each other to identify the scenario that honors the data and hence provides the most accurate representation of the subsurface.

Future work along these lines include separating steam and temperature fronts using density contrast (PP and PS amplitudes as a function of offset could be a useful tool to extract this), and applying this CtL workflow to track the steam movement in time.

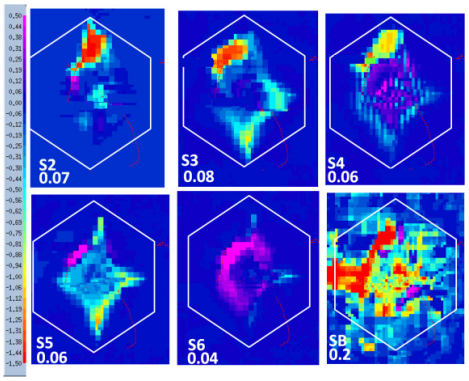

Figure 6: Difference of RRR attribute for all the scenarios and the reference data with no noise. The numbers in the panel reflect the normalized RMS of the difference.

Acknowledgements:

The authors would like to thank Bert-Rik de Zwart for generating the reference reservoir model, scenarios, and valuable discussions. Sincere thanks to Paul Hatchel for his TL codes and Albena Mateeva for her valuable suggestions throughout. The authors would like to thank Shell, PDO and Oman Ministry of Oil and Gas (MOG) for the general collaboration on reservoir surveillance, for their kind permission to publish this paper.

© 2012 SEG

DOI http://dx.doi.org/10.1190/segam2012-0804.1

http://dx.doi.org/10.1190/segam2012-0804.1

EDITED REFERENCES

Note: This reference list is a copy-edited version of the reference list submitted by the author. Reference lists for the 2012 SEG Technical Program Expanded Abstracts have been copy edited so that references provided with the online metadata for each paper will achieve a high degree of linking to cited sources that appear on the Web.

REFERENCES

Fomel, S., and L. Jin, 2009, Time-lapse image registration using the local similarity attribute: Geophysics, **74**, no. 2, A7–A11.

Rocco, G., R. Adawi, F. Kindy, S. Busaidi, S. Farsi, A. Maamari, P. Jorgensen, D. Kiyashchenko, K. Mehta, J. Lopez, and M. Zwaan, 2010, Steam development areal surveillance programme in petroleum development Oman: Proceedings of the EOR Conference at Oil and Gas West Asia, Society of Petroleum Engineers, 129137.

© 2012 SEG

DOI http://dx.doi.org/10.1190/segam2012-0804.1